JOC Article

# Electronic Control of Chiral Quaternary Center Creation in the Intramolecular Asymmetric Heck Reaction

Carl A. Busacca,* Danja Grossbach,† Scot J. Campbell, Yong Dong, Magnus C. Eriksson, Robert E. Harris, Paul-James Jones, Ji-Young Kim, Jon C. Lorenz, Keith B. McKellop, Erin M. O'Brien, Fenghe Qiu, Robert D. Simpson, Lana Smith, Regina C. So, Earl M. Spinelli, Jana Vitous, and Chiara Zavattaro

*Departments of Chemical Development and Analytical Sciences, Boehringer-Ingelheim Pharmaceuticals, Inc., 900 Ridgebury Rd., Ridgefield, Connecticut 06877*

*cbusacca@rdg.boehringer-ingelheim.com*

*Received April 3, 2004*

The Boehringer-Ingelheim phosphinoimidazoline (BIPI) ligands were applied to the formation of chiral quaternary centers in the asymmetric Heck reaction. Several different substrates were examined in detail, using more than 70 members of this new ligand class. Hammett relationships were determined through systematic variation of the ligand electronics. All substrates showed essentially the same Hammett behavior, where enantioselectivity increased as the ligands were made more electron-deficient. Ligand optimization has led to catalysts which give the highest enantioselectivities reported to date for these difficult systems.

## Introduction

The asymmetric Heck reaction (AHR) is a powerful method for the creation of tertiary and quaternary stereocenters via formation of a new C−C bond. Recent reviews[1] document the utility of this reaction in asymmetric synthesis, and it has proven to be an excellent method for the assembly of densely functionalized natural products.[2] The AHR has developed into a very important synthetic tool since the pioneering work of Shibasaki and Overman.[3]

The most successful substrate classes have been those that lead to formation of tertiary stereocenters, particularly the dihydrofurans, dihydropyrroles, and related cyclic olefins. Quaternary centers are more difficult to control and remain an important problem in asymmetric catalysis. The principal ligand classes which have been utilized are the PHOX ligands as employed by Pfaltz and others[4a−e] and BINAP and its derivatives.[4e−k] We have recently reported the application of a new patented ligand class, the BIPI ligands, to chiral quaternary center formation in the AHR.[5] We report here full details of the electronic control of asymmetric induction in four different substrates in this reaction using the BIPI ligands.

## Results and Discussion

The BIPI ligands (Figure 1) were designed so that gross electronic tuning could be achieved by simply varying the nitrogen substituent $R_4$. Alkyl groups in this position lead to strongly basic systems, while acyl and sulfonyl $R_4$ groups lead to more neutral ligands. This type of electronic flexibility is essential if one ligand class is to be

* To whom correspondence should be addressed.

† Current address: Schering AG Process Research, D-13342 Berlin.

(1) (a) Link, J. T. In *Organic Reactions*; Overman, L. E., Ed.; Wiley: New Jersey, 2002; Vol. 60, pp 157−534. (b) Shibasaki, M.; Vogl, E. M. In *Comprehensive Asymmetric Catalysis*; Jacobsen, E. N., Pfaltz, A., Yamamoto, H., Eds.; Springer-Verlag: Heidelberg, 1999; pp 457−487. (c) Shibasaki, M.; Miyazaki, F. In *Handbook of Organopalladium Chemistry for Organic Synthesis*; Negishi, E., Ed.; Wiley: Hoboken, 2002; Vol. 1, pp 1283−1315. (d) Guiry, P. J.; Hennessy, A. J.; Cahill, J. P. *Top. Catal.* **1997**, *4*, 311−326. (e) Shibasaki, M.; Boden, C. D. J.; Kojima, A. *Tetrahedron* **1997**, *53* (22), 7371−7395.

(2) (a) For reviews, see: Dounay, A. B.; Overman, L. E. *Chem. Rev.* **2003**, *103* (8), 2945−2963. (b) Shibasaki, M.; Kojima, A.; Shimizu, S. *J. Heterocycl. Chem*. **1998**, *35* (5), 1057−1064. For recent examples, see: (c) Trost, B. M.; Thiel, O. R.; Tsui, H.-C. *J. Am. Chem. Soc.* **2003**, *125* (43), 13155−13164. (d) Overman, L. E.; Kodanko, J. J. *Angew. Chem., Int. Ed.* **2003**, *42* (22), 2528−2531. (e) Overman, L. E.; Peterson, E. A. *Tetrahedron* **2003**, *59* (35), 6905−6919. (f) Mori, M.; Nakanishi, M.; Kajishima, D.; Sato, Y. *J. Am. Chem. Soc.* **2003**, *125* (32), 9801−9807. (g) Artman, G. D., III; Weinreb, S. M. *Org. Lett.* **2003**, *5* (9), 1523−1526. (h) Trost, B. M.; Tang, W. *Angew. Chem., Int. Ed.* **2002**, *41* (15), 2795−2797. (i) Overman, L. E.; Lebsack, A. D.; Stearns, B. A. *J. Am. Chem. Soc.* **2002**, *124* (31), 9008−9009. (j) Shibasaki, M.; Honzawa, S.; Mizutani, T. *Tetrahedron Lett*. **1999**, *40* (2), 311−314. (k) Overman, L. E.; Matsuura, T.; Poon, D. J. *J. Am. Chem. Soc.* **1998**, *120* (26), 6500−6503.

(3) (a) Shibasaki, M.; Sato, Y.; Sodeoka, M. *J. Org. Chem*. **1989**, *54*, 4738−4739. (b) Overman, L. E.; Carpenter, N. E.; Kucera, D. J. *J. Org. Chem*. **1989**, *54* (25), 5846−5848. (c) Shibasaki, M.; Sodeoka, M. *J. Synth. Org. Chem. Jpn*. **1994**, *52*, 956−957. (d) Overman, L. E. *Pure Appl. Chem*. **1994**, *66*, 1423−1430.

(4) (a) Pfaltz, A.; Loiseleur, O.; Hayashi, M.; Schmees, N. *Synthesis* **1997**, 1338−1345. (b) Loiseleur, O.; Meier, P.; Pfaltz, A. *Angew. Chem., Int. Ed. Engl*. **1996**, *35* (2), 200−202. (c) Hallberg, A.; Ripa, L. *J. Org. Chem*. **1997**, *62* (3), 595−602. (d) Namyslo, J. C.; Kaufmann, D. E. *Chem. Ber*. **1997**, *130* (9), 1327−1331. (e) Guiry, P. J.; Kiely, D. *Tetrahedron Lett*. **2003**, *44* (39), 7377−7380. (f) Ozawa, F.; Hayashi, T. *J. Organomet. Chem*. **1992**, *428*, 267−277. (g) Ozawa, F.; Hayashi, T.; Kubo, A. *Tetrahedron Lett*. **1992**, *33* (11), 1485−1488. (h) Ozawa, F.; Hayashi, T.; Kobatake, Y. *Tetrahedron Lett*. **1993**, *34* (15), 2505−2508. (i) Shibasaki, M.; Kondo, K.; Sodeoka, M. *J. Org. Chem*. **1995**, *60* (14), 4322−4323. (j) Overman, L. E.; Poon, D. J. *Angew. Chem., Int. Ed. Engl*. **1997**, *36* (5), 518−521. (k) Shibasaki, M.; Ohrai, K.; Kondo, K.; Sodeoka, M. *J. Am. Chem. Soc.* **1994**, *116* (26), 11737−11748. (l) Overman, L. E.; Ashimori, A.; Bachand, B.; Poon, D. J. *J. Am. Chem. Soc.* **1998**, *120* (26), 6477−6487.

(5) (a) Busacca, C. A. U.S. Patent 6 316 620, 2001; European Patent 1218388. (b) Busacca, C. A.; Grossbach, D.; So, R. C.; O'Brien, E. M.; Spinelli, E. M. *Org. Lett.* **2003**, *5* (4), 595−598. (c) See also the Supporting Information.

10.1021/jo049448z CCC: $27.50 
Published on Web 07/10/2004

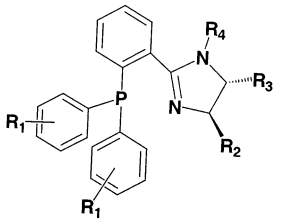


**FIGURE 1.** BIPI ligands.

used successfully for a variety of different asymmetric transformations. This can be illustrated by considering asymmetric hydrogenation and the asymmetric Diels–Alder cycloaddition as simple examples.

Asymmetric hydrogenation of olefins, perhaps the most extensively studied area of asymmetric catalysis, is achieved almost exclusively with electron-rich phosphines and phosphites.[6] These include the very important DIPAMP, DuPhos, DIOP, and Zhang ligands. Asymmetric Diels–Alder cycloadditions, by contrast, are best carried out with neutral or electron-deficient ligands on Lewis acidic metals.[7] No examination of the electronic effects on asymmetric induction in the AHR had been reported, so we chose this transformation to apply the BIPI ligands to. Our approach was simply to determine if electronic trends in enantioselection existed and, if so, to then exploit them.

The ligands were prepared as previously described.[5] Triflate **1** was the first substrate examined. Table 1 collects the results for the first 46 ligands screened for this transformation. The phosphine substituent $R_1$ was systematically varied, while holding $R_2$ and $R_3$ constant as phenyl, and $R_4$ constant as 2-naphthoyl, as shown in entries 1–8. As reported, a Hammett plot of these data proved to be linear with a positive $\rho$ (Figure 3), which was a previously unknown relationship for the AHR. Most importantly, phosphine substituted with 3,5-difluorophenyl (entry 8) gave oxindole **2** in 78% ee, which is significantly higher enantioselectivity than both (*R*)-BINAP (65% ee, (−)) and (S)-*t*-Bu-PHOX (46% ee, (+)) give for this substrate. A similar Hammett scan for the $R_2$/$R_3$ substituents was carried out, as shown in entries 9–21. These ligands were prepared from both $C_2$-symmetric ($R_2 = R_3$) and non-$C_2$-symmetric diamines. The Hammett plot for this series is shown in Figure 4. The Hammett plot for the ligands where $R_2 = R_3$ describes a curve, which goes through a minimum at the neutral H-substituent. Both electron-rich and electron-poor members give increased enantioselectivity. The best substitution for both enantioselectivity and yield was found with the 3,5-difluoro system.

The correlations observed throughout this work are essentially "qualitative" in nature, since we are examining the product of *multiple* reactions (the steps in the catalytic cycle) rather than the *single* reaction examined in classical studies of electronic effects. The Hammett plots are nevertheless a concise representation of the observed electronic effects and the ligand optimization process. For single reactions, curved Hammett plots generally signify a change in mechanism,[8] yet here introduction of the $R_4$ substituent on nitrogen simply breaks the original C2 symmetry of the diamine. In short, the two aryl rings derived from the diamine are now different, and linear behavior for the *sum* of the electronic contributions of these two different rings is not expected in any case. Entries 16–21 were ligands from *non*-$C_2$-symmetric diamines and were created to probe whether the proximal (close to the metal-ligating imine nitrogen) or distal aromatic ring was more important to asymmetric induction. We also hoped to uncover the underlying Hammett behavior of the two individual rings. As shown in Table 1 (and Figure 4), *all* of the ligands where $R_2$ and $R_3$ are different give *lower* enantioselectivities than the sum curve ($R_2 = R_3$), clustering over a small range of log er values, and revealing that the underlying Hammett behavior is definitely nonlinear. Since we had examined only one substrate at this stage, it was difficult to know whether this Hammett behavior was actually significant or largely random, a point which we shall return to shortly.

The $R_4$ substituent was examined next, as shown in entries 22–35 of Table 1. Random Hammett behavior was observed when the *N*-benzoyl para substituent was plotted (not shown), and we concluded that this substituent was too remote to have an effect on enantioselectivity. The behavior of ligands where either the nitrogen substituent or the diamine substituent was alkyl (entries 31–35) proved to be quite interesting. These ligands always gave the *opposite enantiomer* from those ligands derived from aryl diamines or from ligands with electron-withdrawing nitrogen substituents when the absolute stereochemistry was the *same* for each series. We thought that these electronically different ligands might show different metal chelation, so X-ray quality crystals of Pd(II) complexes **3** and **4** were grown. The X-ray crystal structures of these two complexes are shown in Figures 5 and 6. These two metal complexes, which give the *opposite* enantiomer from one another in the AHR, are remarkably similar in their ground-state structures. Both chelate the imine nitrogen, and both have one axial and one equatorial phosphine substituent. Both show an apparent cooperativity between the axial phosphine substituent and one of the imidazoline C-substituents in blocking the alpha face. Each structure shows the *N*-acyl group to be coplanar with the imidazoline ring, and the bond lengths and bond angles between the two are very similar. In summary, the ground-state geometries do not reveal the origin of the reversal in facial selectivity observed.

We were unable to grow high quality crystals of **5** and **6**, so we decided to investigate their metal chelation by

(6) For reviews, see: (a) Zhang, X.; Tang, W. *Chem. Rev.* **2003**, *103* (8), 3029–3069. (b) Brown, J. M. In *Comprehensive Asymmetric Catalysis*; Jacobsen, E. N., Pfaltz, A., Yamamoto, H., Eds.; Springer-Verlag: Heidelberg, 1999; pp 121–182. (c) Halterman, R. L. In *Comprehensive Asymmetric Catalysis*; Jacobsen, E. N., Pfaltz, A., Yamamoto, H., Eds.; Springer-Verlag: Heidelberg, 1999; pp 183–195.

(7) (a) Evans, D. A.; Johnson, J. S. In *Comprehensive Asymmetric Catalysis*; Jacobsen, E. N., Pfaltz, A., Yamamoto, H., Eds.; Springer-Verlag: Heidelberg, 1999; pp 1177–1235.

(8) (a) Cho, B. R.; Kim, N. S.; Kim, Y. K.; Son, K. H. *J. Chem. Soc., Perkin Trans. 2* **2000**, *7*, 1419–1423. (b) Kevill, D. K.; Wang, W. K. F. *J. Chem. Soc., Perkin Trans. 2* **1998**, *12*, 2631–2638. (c) Bauld, N. L.; Yueh, W. *J. Chem. Soc., Perkin Trans. 2* **1996**, *8*, 1761–1766. (d) Petnehazy, I.; Clementis, G.; Jaszay, Z. M.; Toke, L.; Hall, C. D. *J. Chem. Soc., Perkin Trans. 2* **1996**, *11*, 2279–2284. (e) Wayner, D. D. M.; Huang, Y. *J. Am. Chem. Soc.* **1994**, *116* (5), 2157–2158. (f) Drago, R. S.; Zoltewicz, J. A. *J. Org. Chem.* **1994**, *59* (10), 2824–2830. (g) Richard, J. P.; Amyes, T. L. *J. Am. Chem. Soc.* **1990**, *112* (26), 9507–9512.

**TABLE 1. Triflate 1, Ligand Screening Set**

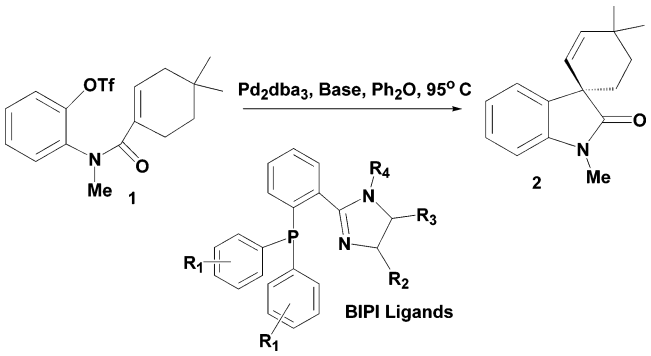


| entry | $R_1$ | $R_2$ | $R_3$ | $R_4$ | base | yield, % | ee, % |
|---|---|---|---|---|---|---|---|
| 1 | 4-OMe | (*R*)-Ph | (*R*)-Ph | 2-naphthoyl | PMP[a] | 15 | 39.9 (−) |
| 2 | 4-Me | (*R*)-Ph | (*R*)-Ph | 2-naphthoyl | PMP | 15 | 54.5 (−) |
| 3 | 3,5-$Me_2$ | (*R*)-Ph | (*R*)-Ph | 2-naphthoyl | PMP | 82 | 49.9 (−) |
| 4 | H | (*S*)-Ph | (*S*)-Ph | 2-naphthoyl | PMP | 68 | 44.6 (+) |
| 5 | 4-F | (*R*)-Ph | (*R*)-Ph | 2-naphthoyl | PMP | 68 | 53.3 (−) |
| 6 | 4-Cl | (*R*)-Ph | (*R*)-Ph | 2-naphthoyl | PMP | 30 | 66.1 (−) |
| 7 | 4-$CF_3$ | (*R*)-Ph | (*R*)-Ph | 2-naphthoyl | PMP | 25 | 72.9 (−) |
| 8 | 3,5-$F_2$ | (*S*)-Ph | (*S*)-Ph | 2-naphthoyl | PMP | 39 | **78.1 (+)** |
| 9 | H | (*S*)-(4-OMePh) | (*S*)-(4-OMePh) | 2-naphthoyl | PMP | 13 | 51.6 (+) |
| 10 | H | (*R*)-(4-MePh) | (*R*)-(4-MePh) | 2-naphthoyl | PMP | 25 | 45.2 (−) |
| 11 | H | (*S*)-(3,5-$Me_2$Ph) | (*S*)-(3,5-$Me_2$Ph) | 2-naphthoyl | PMP | 85 | 46.7 (+) |
| 12 | H | (*S*)-(4-FPh) | (*S*)-(4-FPh) | 2-naphthoyl | PMP | 61 | 48.3 (+) |
| 13 | H | (*S*)-(4-ClPh) | (*S*)-(4-ClPh) | 2-naphthoyl | PMP | 17 | 61.5 (+) |
| 14 | H | (*R*)-(4-$CF_3$Ph) | (*R*)-(4-$CF_3$Ph) | 2-naphthoyl | PMP | 12 | 64.6 (−) |
| 15 | H | (*S*)-(3,5-$F_2$Ph) | (*S*)-(3,5-$F_2$Ph) | 2-naphthoyl | PMP | 93 | 62.7 (+) |
| 16 | H | (*S*)-Ph | (*S*)-(4-OMePh) | 2-naphthoyl | PMP | 75 | 41.4 (+) |
| 17 | H | (*S*)-(4-OMePh) | (*S*)-Ph | 2-naphthoyl | PMP | 73 | 40.8 (+) |
| 18 | H | (*S*)-Ph | (*S*)-(4-OMsPh) | 2-naphthoyl | PMP | 70 | 58.2 (+) |
| 19 | H | (*S*)-(4-OMsPh) | (*S*)-Ph | 2-naphthoyl | PMP | 86 | 47.8 (+) |
| 20 | H | (*S*)-Ph | (*S*)-(4-$CO_2$MePh) | 2-naphthoyl | PMP | 65 | 40.9 (+) |
| 21 | H | (*S*)-(4-$CO_2$MePh) | (*S*)-Ph | 2-naphthoyl | PMP | 57 | 42.6 (+) |
| 22 | H | (*S*)-Ph | (*S*)-Ph | 1-naphthoyl | PMP | 85 | 40.6 (+) |
| 23 | H | (*R*)-Ph | (*R*)-Ph | 4-$NMe_2$-Bz | PMP | 25 | 37.0 (−) |
| 24 | H | (*S*)-Ph | (*S*)-Ph | 4-OMe-Bz | PMP | 27 | 47.6 (+) |
| 25 | H | (*R*)-Ph | (*R*)-Ph | 4-Me-Bz | PMP | 81 | 32.7 (−) |
| 26 | H | (*S*)-Ph | (*S*)-Ph | Bz | PMP | 76 | 42.2 (+) |
| 27 | H | (*R*)-Ph | (*R*)-Ph | 4-Cl-Bz | PMP | 71 | 40.1 (−) |
| 28 | H | (*R*)-Ph | (*R*)-Ph | 4-$OCF_3$-Bz | PMP | 88 | 33.7 (−) |
| 29 | H | (*R*)-Ph | (*R*)-Ph | 4-$CF_3$-Bz | PMP | 90 | 41.9 (−) |
| 30 | H | (*S*)-Ph | (*S*)-Ph | 4-CN-Bz | PMP | 83 | 36.6 (+) |
| 31 | H | (*S*)-Ph | (*S*)-Ph | methyl | PMP | 17 | 20.5 (−)[b] |
| 32 | H | (*S*)-Ph | (*S*)-Ph | benzyl | PMP | 16 | 11.9 (−)[b] |
| 33 | H | CDA[c] | CDA[c] | acetyl | PMP | 18 | 36.7 (−) |
| 34 | H | (*R*)-$(CH_2)_4$- | (*R*)-$(CH_2)_4$- | acetyl | PMP | 21 | 29.2 (+) |
| 35 | H | (*S*)-*t*-Bu | (*S*)-*t*-Bu | acetyl | PMP | 88 | 29.1 (−) |
| 36 | 4-Cl | (*R*)-3,5-$F_2$Ph | (*R*)-3,5-$F_2$Ph | 2-naphthoyl | PMP | 25 | **80.6 (−)** |
| 37 | 4-Cl | (*R*)-3,5-$F_2$Ph | (*R*)-3,5-$F_2$Ph | 4-OMe-Bz | PMP | 28 | **78.2 (−)** |
| 38 | 4-Cl | (*R*)-3,5-$F_2$Ph | (*R*)-3,5-$F_2$Ph | 4-$CF_3$-Bz | PMP | 26 | **74.9 (−)** |
| 39 | 4-Cl | (*R*)-3,5-$F_2$Ph | (*R*)-3,5-$F_2$Ph | 2-naphthoyl | (*R*)-CEP[d] | 51 | **79.3 (−)** |
| 40 | 4-Cl | (*R*)-3,5-$F_2$Ph | (*R*)-3,5-$F_2$Ph | 2-naphthoyl | (*S*)-CEP[e] | 48 | **78.8 (−)** |
| 41 | 4-Cl | (*R*)-3,5-$F_2$Ph | (*R*)-3,5-$F_2$Ph | 2-naphthoyl | (*R*,*S*)-Pin[f] | 51 | **76.4 (−)** |
| 42 | 4-Cl | (*R*)-3,5-$F_2$Ph | (*R*)-3,5-$F_2$Ph | 2-naphthoyl | (*S*,*R*)-Pin[g] | 45 | **79.0 (−)** |
| 43 | 4-Cl | (*R*)-3,5-$F_2$Ph | (*R*)-3,5-$F_2$Ph | 2-naphthoyl | PS[h] | NR | NA |
| 44 | 4-Cl | (*R*)-3,5-$F_2$Ph | (*R*)-3,5-$F_2$Ph | 2-naphthoyl | Quin[i] | NR | NA |
| 45 | 3,5-$F_2$Ph | (*R*)-3,5-$F_2$Ph | (*R*)-3,5-$F_2$Ph | 2-naphthoyl | PMP | 38 | **87.6 (−)** |
| 46 | 3,5-$F_2$Ph | (*R*)-3,5-$F_2$Ph | (*R*)-3,5-$F_2$Ph | 2-naphthoyl | (*S*)-CEP[e] | 50 | **86.8 (−)** |

[a] Pentamethylpiperidine. [b] DMA as solvent. [c] (1*R*,2*S*,3*R*)-camphordiamine. [d] (*R*)-1-(1′-cyclohexylethyl)pyrrolidine. [e] (*S*)-1-(1′-cyclohexylethyl)pyrrolidine. [f] (*R*,*R*,*R*,*S*)-pinanepyrrolidine. [g] (*S*,*S*,*S*,*R*)-pinanepyrrolidine. [h] Proton Sponge. [i] Quinuclidine. Chiralcel OD, 8.70 min (+), 9.8 min (−).

means of NMR. Isotopically labeled ligands were prepared as previously described by first synthesizing 1,2-diphenylethylenediamine from benzil using $^{15}NH_4OAc$. Imidazoline formation and nitrogen substitution completed the synthesis. We also introduced $^{13}C$-labeled nitrogen substituents by using $^{13}CH_3I$ and $CH_3{}^{13}COCl$, respectively. The isotopically labeled free ligands and Pt(II) complexes (**7** and **8**) were then examined by $^{15}N$, $^{13}C$, and $^{31}P$ NMR. We chose Pt(II) rather than Pd(II) to avoid the quadrupolar line broadening observed with the latter metal. The NMR data are summarized in Figure 2.

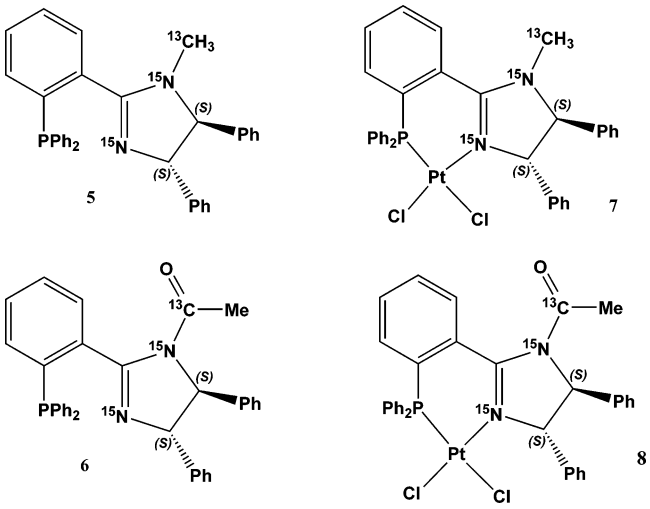


**FIGURE 2.** Isotopically labeled species. **5**. $^{15}$N NMR $\delta$: −145.52 (*N*-im), −275.31 ($^1J_{N-C}$ = 9.3 Hz, *N*-Me). $^{31}$P NMR $\delta$: −11.13. $^{13}$C NMR $\delta$: 33.38 (*C*H$_3$, dd, $J$ = 3.3, 9.2 Hz). $^1$H NMR $\delta$: 4.87 (C*H*N-im), 4.23 (C*H*N-Me). **7**. $^{15}$N NMR $\delta$: −249.54 (*N*-im) −276.06 ($^1J_{N-C}$ = 9.7 Hz, *N*-Me). $^{31}$P NMR $\delta$: 3.85 ($^1J_{P-Pt}$ = 3791 Hz). $^{13}$C NMR $\delta$: 38.01 (*C*H$_3$, d, $^1J_{C-N}$ = 10.0 Hz). $^1$H NMR $\delta$: 6.12 (C*H*N-im), 4.31 (C*H*N-Me). **6**. $^{15}$N NMR $\delta$: −119.98 (*N*-im), −202.26 ($^1J_{N-C}$ = 9.3 Hz, *N*-Ac). $^{31}$P NMR $\delta$: −11.95. $^{13}$C NMR $\delta$: 168.22 (*C*O, d, $^1J_{C-N}$ = 10.3 Hz), 24.77 (*C*H$_3$, dd, $J$ = 5.6, 52.7 Hz). $^1$H NMR $\delta$: 5.22 (C*H*N-Ac), 5.08 (C*H*N-im). **8**. $^{15}$N NMR $\delta$: −203.29 (*N*-im), −214.52 ($^1J_{N-C}$ = 9.7 Hz, *N*-Ac). $^{31}$P NMR $\delta$: 3.71 ($^1J_{P-Pt}$ = 3665 Hz). $^{13}$C NMR $\delta$: 169.51 (*C*O, d, $^1J_{C-N}$ = 7.5 Hz), 24.14 (*C*H$_3$, dd, $J$ = 8.8, 53.9 Hz). $^1$H NMR $\delta$: 6.77 (C*H*N-im), 5.13 (CHN-Ac).

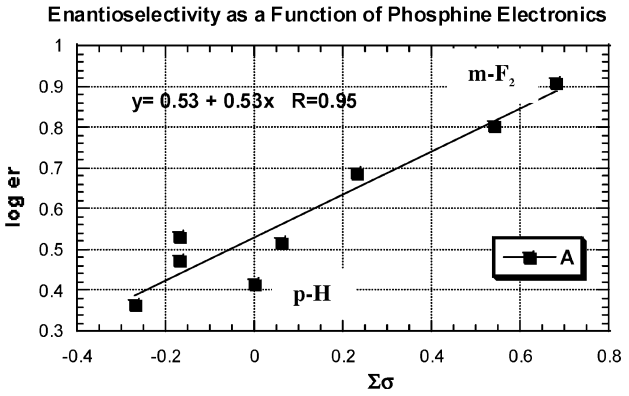


**FIGURE 3.** Phosphine Hammett plot, oxindole **2**.

A comparison of the NMR data for free ligand **5** and platinum complex **7** is informative. The N-Me resonance appears as a doublet in $^{15}$N due to coupling with the attached $^{13}$C nucleus. This $^{15}$N resonance shifts less than one ppm upon complexation, while the imine resonance moves 104 ppm upfield in the complex. Similar shieldings of late transition metal bound nitrogen resonances have been previously observed.[9] This unambiguously establishes the chelating nitrogen as the imine. Chelation of the imine nitrogen in platinum complex **8** was also determined by comparison of the $^{15}$N data for the free (**6**) and bound species.

Inspection of Figure 2 shows that the *N*-imine $^{15}$N signal moves upfield by 82 ppm in this platinum complex (**8**). The phosphorus resonances are deshielded by ~15 ppm in both complexes relative to the free ligands. The

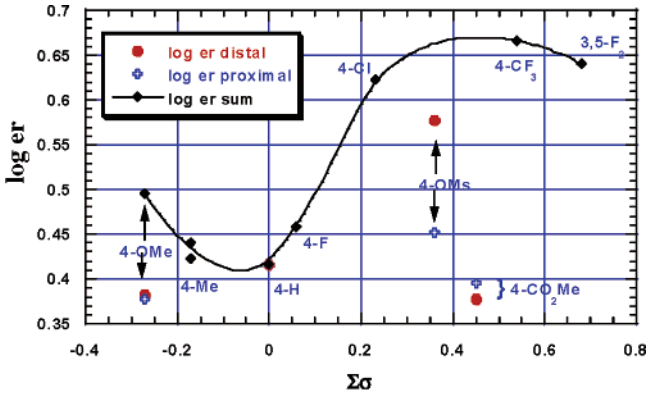


**FIGURE 4.** Diamine Hammett plot, oxindole **2**.

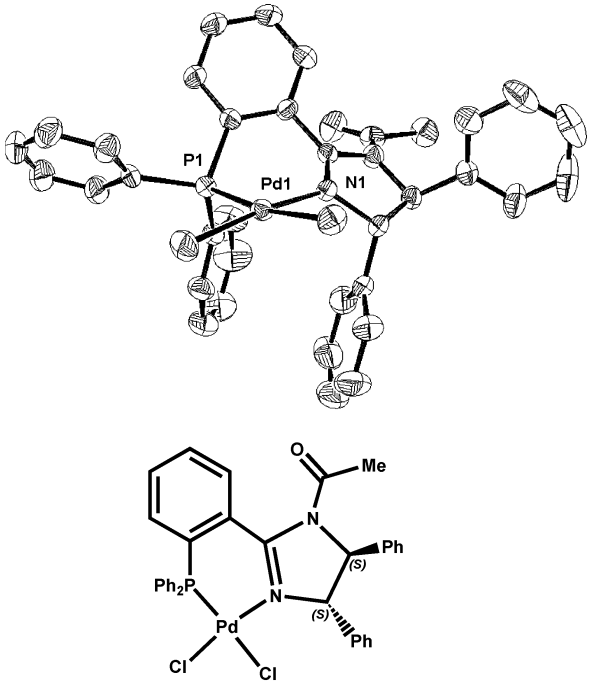


**FIGURE 5.** ORTEP plot of complex **3**. Selected bond lengths (Å) and angles (deg): Pd−P, 2.232; Pd−N(1), 2.046; P−Pd−N(1), 86.27°; P−Pd−Cl(1), 93.36°; N−Pd−Cl(2), 89.54°; Cl(1)−Pd−Cl(2), 91.87°.

methine imidazoline protons proximal to the chelating nitrogen in both complexes are strongly deshielded (ca. 1.5 ppm) relative to the free ligands, while the distal methines are essentially unchanged. In contrast, both proximal and distal methine $^{13}$C resonances are minimally affected (1−3 ppm upfield shift) by complexation. The NMR data for all structures examined thus show that only the imine nitrogens are involved in metal chelation.

An examination of entries 33−35 of Table 1 provides critical insight into the requirements for asymmetric induction in this substrate. The two most sterically hindered diamines used were bis-*tert*-butyl ethylenedi-

(9) (a) Schenetti, L.; Mucci, A.; Longato, B. *J. Chem. Soc., Dalton Trans.* **1996**, *3*, 299−303. (b) Bissinger, H.; Beck, W. *Z. Naturforsch., Teil B* **1985**, *40B* (4), 507−511. (c) Longato, B.; Schenetti, L.; Bandoli, G.; Dolmella, A.; Trovo, G. *Inorg. Chem.* **1994**, *33* (14), 3169−3176. (d) Longato, B.; Pasquato, L.; Mucci, A.; Schenetti, L. *Eur. J. Inorg. Chem.* **2003**, *1*, 128−137.

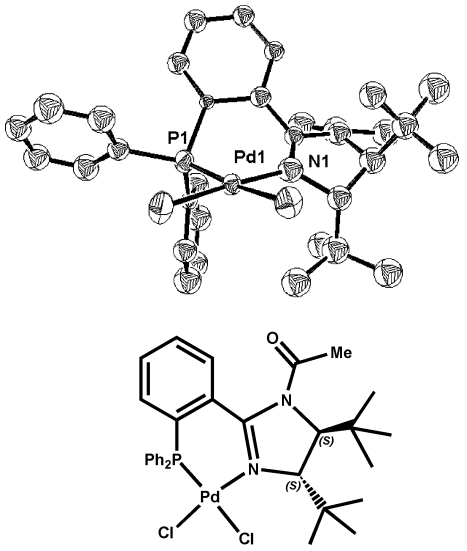


**FIGURE 6.** ORTEP plot of complex **4**. Selected bond lengths (Å) and angles (deg): Pd−P, 2.231; Pd−N(1), 2.083; P−Pd−N(1), 86.8°; P−Pd−Cl(2), 91.5°; N−Pd−Cl(1), 91.3°; Cl(1)−Pd−Cl(2), 90.7°.

amine and camphordiamine, used to make the ligands in entries 33 and 35. Each gives only very modest enantioselectivity (37%, 29% ee). The *least* sterically hindered diamine used was 1,2-cyclohexanediamine, in entry 34. This ligand furnished oxindole **2** also with 29% ee. Clearly there is little steric contribution to asymmetric induction in this substrate, while electronic effects (e.g., Figure 3) are operative. We completed the initial screening set for substrate **1** by combining the best phosphines (4-chlorophenyl and 3,5-difluorophenyl) and diamine substitution (3,5-difluorophenyl) and varied $R_4$ between three electron-withdrawing groups. The chlorophosphine results (entries 36−38) gave **2** with 75−81% ee, with 2-naphthoyl as the optimum $R_4$ group. The difluorophenyl phosphine result (entry 45) gave the highest enantioselectivity observed, 88% ee.

The isolated yield of **2** after 18 h for most of the electron-deficient ligand systems were reduced relative to their more neutral analogues. We therefore undertook a screening of bases, since choice of base has been reported to affect enantioselectivity and yield.[4f−h,l,10] To the best of our knowledge, chiral bases have never been applied to the asymmetric Heck reaction, so we prepared the four chiral amines **10**−**13** as shown in Scheme 1 for evaluation as well. The commercially available optically pure primary amines were converted to their pyrrolidine derivatives with 1,4-dibromobutane using the procedure of Li.[11] A total of six additional bases, as shown in entries 39−44, were evaluated. Both Proton Sponge and quinuclidine led to a catalytically inactive system (entries 43−44). The enantiomeric bases **10**−**13** were evaluated in four side-by-side experiments (entries 39−42). All four bases provided higher isolated yields of **2** after our 18 h reaction time, yet there was no significant effect on enantioselectivity, as all furnished **2** in 76−79% ee. Base

**SCHEME 1. Synthesis of Chiral Tertiary Amines**

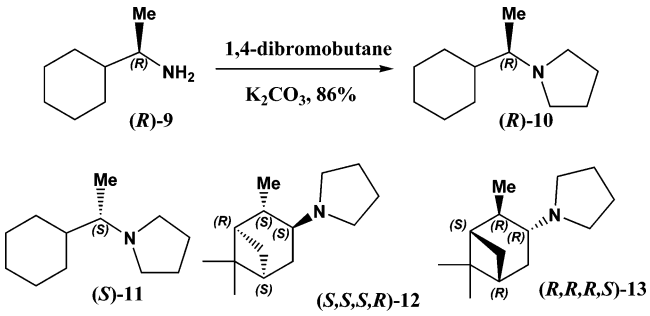


**11** was used with our most optimized ligand, as shown in entry 46. Isolated yield was once again improved, and the enantioselectivity changed by less than 1% relative to the use of PMP as base. These small changes in ee are about the reproducibility in enantioselectivity from one experiment to the next. Choice of base can clearly improve catalytic efficiency in these systems, however. In all examples from Table 1 (as well as all following Heck reaction tables), the reaction yield based on recovered starting material was nearly quantitative, since unreacted triflate could be isolated in all cases of incomplete conversion. No degradation of starting material was observed, although a general trend of lower reaction conversion was found with strongly electron-rich or electron-deficient ligands. This trend could be partially offset by meta disposition of ligand aryl substituents, however. This behavior is well illustrated by comparing entries 14 and 15 of Table 1. The *p*-trifluoromethyl and *m*-difluoro substituted ligands give nearly identical enantioselectivities (65% vs 63%) as would be expected from their similar Hammett values. However, the meta-disubstituted ligand furnishes oxindole **2** in high yield (93%), while the para-substituted system gives only 13% product after the same 18 h reaction time.

We next examined triflate **14**, our second substrate, which was prepared in a manner analogous to triflate **1**.[5b,c] The results of ligand screening are collected in Table 2.

Two striking observations were immediately made when comparing Table 2 to Table 1: The second substrate gives much higher isolated yields accompanied by much lower enantioselectivity than the first substrate. The phosphine and diamine Hammett plots for the second substrate are shown in Figures 7 and 8, respectively.

Figure 7 shows a diminished linear correlation relative to the first substrate, and the ee's span a smaller range. The overall trend is the same, however, with a positive $\rho$ and 3,5-difuorophenyl as the best phosphine substitution. The diamine Hammett plot in Figure 8 is remarkably similar to that of the first substrate (Figure 4). The sum curve defining the $R_2 = R_3$ ligands again goes through a minimum near the neutral hydrogen substituent, and both more electron-rich and electron-poor species give higher enantioselectivity. Even the relative position of the ligands derived from the non-$C_2$-symmetric diamines are the same as the first substrate, once again falling below the sum curve, and showing the same rank ordering of the proximal and distal methoxy pair, where the largest difference in log er was seen. In agreement with the phosphine data for this substrate,

(10) Lloyd-Jones, G. C.; Slatford, P. A. *J. Am. Chem. Soc.* **2004**, *126* (9), 2690−2691.
(11) Li, Z.; Upadhyay, V.; DeCamp, A. E.; DiMichele, L.; Reider, P. J. *Synthesis* **1999**, Suppl. 1, 1453−1458.

**TABLE 2. Triflate 14, First Ligand Screening Set**

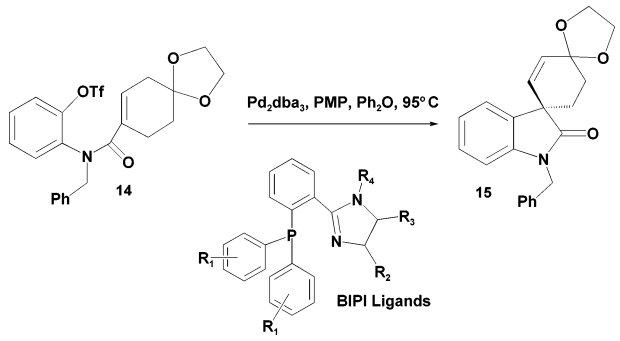


| entry | $R_1$ | $R_2$ | $R_3$ | $R_4$ | yield, % | ee,[a] % |
|---|---|---|---|---|---|---|
| 1 | 4-OMe | (*R*)-Ph | (*R*)-Ph | 2-naphthoyl | 65 | 2.3 (*R*) |
| 2 | 4-Me | (*R*)-Ph | (*R*)-Ph | 2-naphthoyl | 60 | 10.9 (*R*) |
| 3 | 3,5-$Me_2$ | (*R*)-Ph | (*R*)-Ph | 2-naphthoyl | 71 | 16.2 (*R*) |
| 4 | H | (*S*)-Ph | (*S*)-Ph | 2-naphthoyl | 98 | 6.6 (*S*) |
| 6 | 4-Cl | (*R*)-Ph | (*R*)-Ph | 2-naphthoyl | 89 | 17.7 (*R*) |
| 7 | 4-$CF_3$ | (*R*)-Ph | (*R*)-Ph | 2-naphthoyl | 97 | 17.7 (*R*) |
| 8 | 3,5-$F_2$ | (*S*)-Ph | (*S*)-Ph | 2-naphthoyl | 89 | 31.1 (*S*) |
| 9 | H | (*S*)-(4-OMePh) | (*S*)-(4-OMePh) | 2-naphthoyl | 46 | 13.0 (*S*) |
| 10 | H | (*R*)-(4-MePh) | (*R*)-(4-MePh) | 2-naphthoyl | 87 | 0.6 (*R*) |
| 11 | H | (*S*)-(3,5-$Me_2$Ph) | (*S*)-(3,5-$Me_2$Ph) | 2-naphthoyl | 86 | 4.5 (*S*) |
| 12 | H | (*S*)-(4-ClPh) | (*S*)-(4-ClPh) | 2-naphthoyl | 81 | 25.9 (*S*) |
| 13 | H | (*R*)-(4-$CF_3$Ph) | (*R*)-(4-$CF_3$Ph) | 2-naphthoyl | 79 | 32.6 (*R*) |
| 14 | H | (*S*)-(3,5-$F_2$Ph) | (*S*)-(3,5-$F_2$Ph) | 2-naphthoyl | 95 | 31.4 (*S*) |
| 15 | H | (*S*)-Ph | (*S*)-(4-OMePh) | 2-naphthoyl | 85 | 5.4 (*S*) |
| 16 | H | (*S*)-(4-OMePh) | (*S*)-Ph | 2-naphthoyl | 46 | 7.8 (*S*) |
| 17 | H | (*S*)-Ph | (*S*)-(4-OMsPh) | 2-naphthoyl | 64 | 23.8 (*S*) |
| 18 | H | (*S*)-(4-OMsPh) | (*S*)-Ph | 2-naphthoyl | 57 | 8.4 (*S*) |
| 19 | H | (*S*)-Ph | (*S*)-(4-$CO_2$MePh) | 2-naphthoyl | 84 | 13.9 (*S*) |
| 20 | H | (*S*)-(4-$CO_2$MePh) | (*S*)-Ph | 2-naphthoyl | 86 | 13.0 (*S*) |
| 21 | H | (*S*)-*t*-Bu | (*S*)-*t*-Bu | acetyl | 82 | 50.9 (*R*) |
| 22 | 4-Cl | (*R*)-(3,5-$F_2$Ph) | (*R*)-(3,5-$F_2$Ph) | 2-naphthoyl | 81 | 55.9 (*R*) |
| 23 | 3,5-$F_2$ | (*R*)-(3,5-$F_2$Ph) | (*R*)-(3,5-$F_2$Ph) | 2-naphthoyl | 67 | **77.5** (*R*) |

[a] Chiralcel OD, 13.8 min (*S*)-(−), 17.6 min (*R*)-(+).

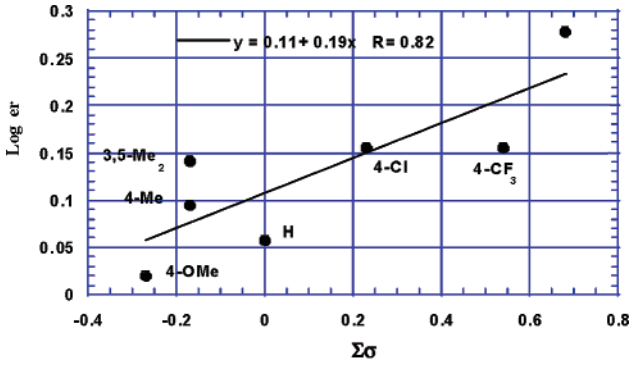


**FIGURE 7.** Phosphine Hammett plot, oxindole **15**.

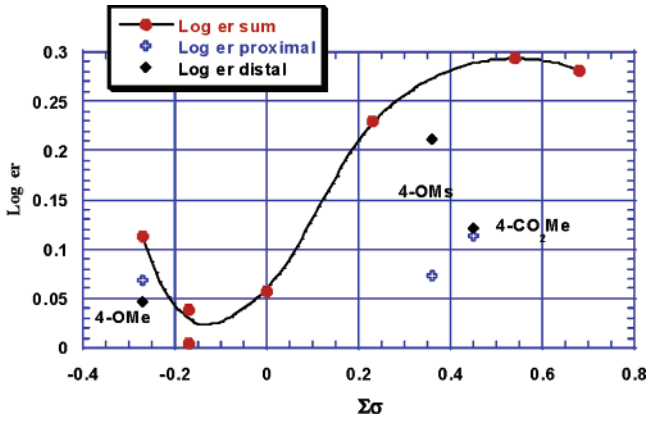


**FIGURE 8.** Diamine Hammett plot, oxindole **15**.

the Hammett plot is "compressed": the shape is the same, yet the range of ee's spanned is reduced. Fortunately, combining the optimized phosphine and diamine substitution patterns still leads to a ligand with good enantioselectivity, as shown in entry 23 of Table 2. This optimized ligand furnishes oxindole **15** in 78% ee and 67% yield after 18 h. It seems the synergistic effect between the optimized phosphine and diamine substituents is more pronounced for this substrate than for triflate **1**. We observed 23% ee (*S*) using (*R*)-*t*-Bu-PHOX for this substrate, as determined by chiral HPLC. Overman has reported 66% ee (*R*) for this substrate with (*R*)-BINAP, using chiral shift reagent NMR determination of enantioselection.[41] We observed 45% ee using (*R*)-BINAP with chiral HPLC analysis for this substrate.

The increased catalytic efficiency for this ketal substrate is quite intriguing, since it applies to all ligands, irrespective of their electronics. Both the nitrogen substituent and the olefin were changed relative to the first substrate, however, so we needed to prepare another substrate to probe which structural change was responsible for the increased yield. As shown in Table 3, *N*-methyl triflate **16** (prepared by methods analogous to

**TABLE 3. Triflate 16, Selected Ligand Screening**

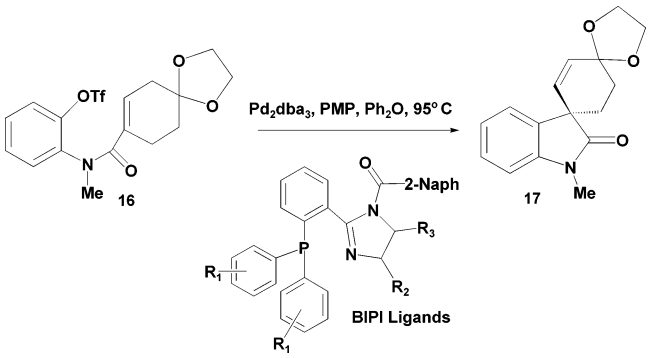


| entry | $R_1$ | $R_2$ | $R_3$ | yield (%) | ee[a], % |
|---|---|---|---|---|---|
| 1 | H | (*S*)-4-ClPh | (*S*)-4-ClPh | 68 | 52.1 (*R*) |
| 2 | 4-Cl | (*R*)-Ph | (*R*)-Ph | 80 | 62.7 (*S*) |
| 3 | 3,5-$F_2$ | (*S*)-Ph | (*S*)-Ph | 99 | 69.9 (*R*) |
| 4 | 3,5-$F_2$ | (*R*)-3,5-$F_2$Ph | (*R*)-3,5-$F_2$Ph | 53 | **82.8** (*S*) |

[a] Chiralpak AD, 7.70 min (*S*)-(+), 8.97 min (*R*)−(−).

those already described[5b,c]) was then screened against a select group of ligands.

The yields of oxindole **17** found with all four electron-deficient ligands for this *N*-methyl ketal substrate were significantly higher than the *N*-methyl-*gem*-dimethyl substrate **1** and behaved like ketal substrate **14** in terms of catalytic efficiency. The enantioselectivities observed with substrate **16**, however, were much higher than for ketal **14**, particularly for the ligands optimized in only one region (Table 3, entries 1−3). We were able to make two critical conclusions from these data. First, the ketal moiety of the substrates imparts increased catalytic efficiency, without affecting enantioselectivity. Second, the *N*-benzyl group tends to give lower enantioselectivities than the analogous *N*-methyl Heck substrates. We believe this could have important implications in the use of the asymmetric Heck reaction for synthesis of complex tragets. As seen here, the ketal and nitrogen substituent of the substrate might play the role of protecting groups in a total synthesis. Their judicious choice prior to the asymmetric Heck reaction could allow for increased enantioselectivity without sacrifice of catalytic efficiency.

Several lines of evidence generated here point to facilitated $\beta$-hydride elimination as the source of the greater catalytic efficiency: (1) Base choice can have dramatic effects on turnover, as shown in Table 1. (2) No significant differences in enantioselection were observed between two pairs of enantiomeric strong bases, suggesting, as expected, that the step they are involved in is not the enantiodifferentiating step. (3) The ketal substrates give better turnover than their alkyl analogue, irrespective of the nitrogen substituent. (4) The increased catalytic efficiency seen with the ketals is seen over the entire range of ligand electronics, for all ligand members. Since electronic effects on enantioselection are operative, it is unlikely that the source of increased turnover is electronic in origin.

Application of our optimized ligand (Table 3, entry 4) to substrate **16** furnished **17** in 83% ee and 53% yield after 18 h. We observed 23% ee (*S*) for (*R*)-*t*-Bu-PHOX for this substrate, as determined by chiral HPLC. Overman has reported 71% ee (*S*) for this substrate with (*S*)-BINAP, using chiral shift reagent NMR determination of enantioselection.[4l] We observed ∼40% ee for this substrate using (*S*)-BINAP with chiral HPLC analysis of the product. As was observed for the first substrates, the optimized BIPI ligands give substantially higher enantioselectivities with substrate **16** than do BINAP or *t*-Bu-PHOX.

**TABLE 4. Triflate 18, Selected Ligand Screening**

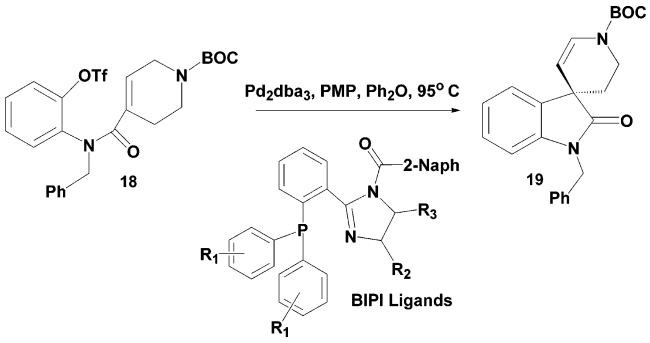


| entry | $R_1$ | $R_2$ | $R_3$ | yield, % | ee,[a] % |
|---|---|---|---|---|---|
| 1 | H | (*S*)- Ph | (*S*)- Ph | 83 | 21.4 (−) |
| 2 | 4-OMe | (*R*)-Ph | (*R*)-Ph | 70 | 11.4 (+) |
| 3 | 4-Cl | (*R*)-Ph | (*R*)-Ph | 85 | 39.4 (+) |
| 4 | 4-$CF_3$ | (*R*)-Ph | (*R*)-Ph | 71 | **46.9** (+) |
| 5 | 3,5-$F_2$ | (*S*)- Ph | (*S*)- Ph | 88 | 29.8 (−) |
| 6 | H | (*S*)-4-OMePh | (*S*)-4-OMePh | 44 | 15.7 (−) |
| 7 | H | (*R*)-4-MePh | (*R*)-4-MePh | 83 | 23.6 (+) |
| 8 | H | (*S*)-4-FPh | (*S*)-4-FPh | 51 | 32.0 (−) |
| 9 | H | (*S*)-4-ClPh | (*S*)-4-ClPh | 58 | 34.1 (−) |
| 10 | H | (*S*)-3,5-$F_2$Ph | (*S*)-3,5-$F_2$Ph | 68 | 35.0 (−) |
| 11 | 3,5-$F_2$ | (*R*)-3,5-$F_2$Ph | (*R*)-3,5-$F_2$Ph | 62 | 35.6 (+) |
| 12 | 4-Cl | (*R*)-3,5-$F_2$Ph | (*R*)-3,5-$F_2$Ph | 25 | 41.5 (+) |
| 13 | 4-$CF_3$ | (*S*)-3,5-$F_2$Ph | (*S*)-3,5-$F_2$Ph | 11 | **50.1** (−) |

[a] Chiralcel OD, 11.40 min (+), 14.9 min (−).

Our final substrate examined for the asymmetric Heck reaction was triflate **18** bearing the protected tetrahydropyridine functionality.[5b,c] We chose this substrate as a reasonable model for a number of natural products which possess the spiropiperidine functionality.[12] Since the olefin portion of this triflate was significantly different than the other substrates, we again screened against a sufficient number of ligands to allow generation of the phosphine and diamine Hammett plots. The data are collected in Table 4, and the Hammett plots are shown in Figures 9 and 10. The Hammett behavior for this substrate differs from all of the other substrates in at least three ways: (1) 3,5-difluorophosphine substitution is not the most enantioselective, (2) the diamine Hammett shows a general increase in enantioselectivity with increasing $\Sigma\sigma$ without the clear minimum in the plot previously seen, and (3) ligands optimized in both regions (entries 11−13, Table 4) do not show the dramatic increases in enantioselectivity previously observed. We examined (*R*)-BINAP/n-BuNBr and (*R*)-*t*-Bu-PHOX against this substrate and initially found no reaction with either ligand after 24 h at 95 °C. Triflate **18** could be recovered quantitatively from the PHOX experiment, while **18** was consumed with BINAP. The BINAP experiment was then

(12) (a) Ariza, M. R.; Larsen, T. O.; Petersen, B. O.; Duus, J. O.; Christophersen, C.; Barrero, A. F. *J. Nat. Prod.* **2001**, *64* (12), 1590−1592. (b) Larsen, T. O.; Frydenvang, K.; Frisvad, J. C.; Christophersen, C. *J. Nat. Prod.* **1998**, *61* (9), 1154−1157.

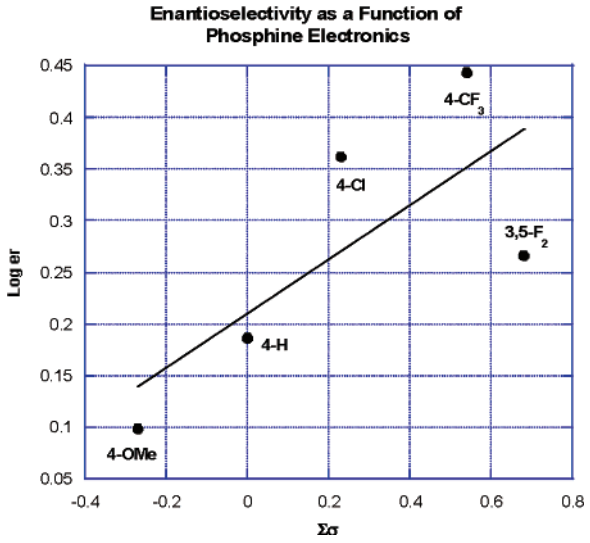


**FIGURE 9.** Phosphine Hammett plot, oxindole **19**.

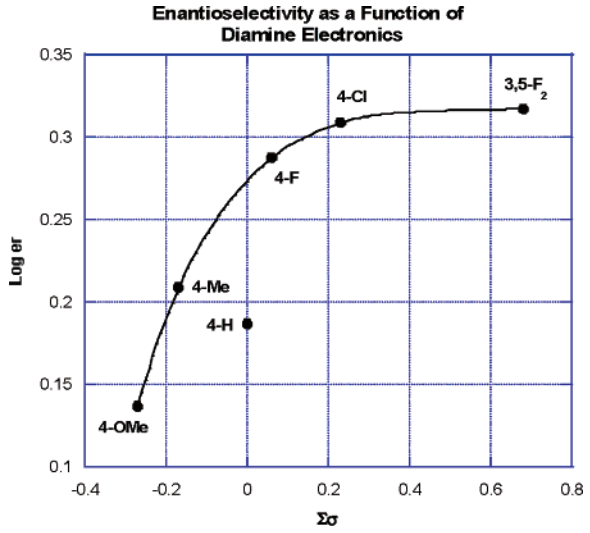


**FIGURE 10.** Diamine Hammett plot, oxindole **19**.

repeated, and aliquots were withdrawn at 2 h intervals. No cyclization product **19** was ever formed, yet the triflate was consumed in about 6 h, generating polar impurities. Triflate **18** is clearly unstable under these reaction conditions. The PHOX experiment was then repeated at 120 °C, and enecarbamate oxindole **19** could then be isolated in 54% yield, with an ee of 46.2% (+). The optimized BIPI ligands (entries 4 and 13) are thus somewhat more enantioselective than the PHOX ligand, although only the *p*-trifluoromethyl ligand (entry 4) is practical in terms of yield. It is interesting to note that the same rank ordering of phosphine substituents (*p*-$CF_3$ > *p*-Cl > *m*-$F_2$) with respect to enantioselectivity observed in the phosphine Hammett plot of Figure 9 is maintained in the optimized ligands, entries 11−13. It is clear that tetrahydropyridines such as **18** are still quite challenging substrates for the asymmetric Heck reaction.

We wished to briefly examine the one ligand region not previously studied—the central benzo ring. Using the nomenclature previously introduced, this region was designated $R_5$. We decided to vary only $R_5$ first, while

**TABLE 5. Trifate 1, $R_5$ Screening Set**

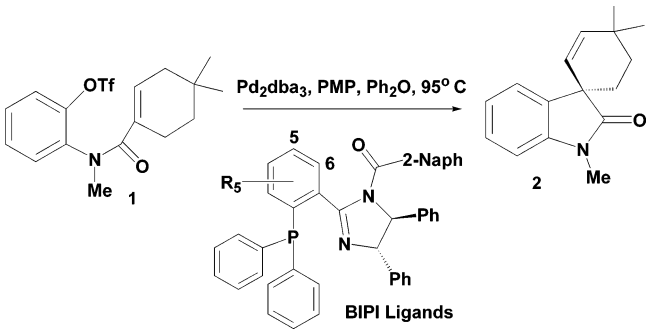


| entry | $R_5$ | yield, % | ee,[b] % |
|---|---|---|---|
| 1 | H | 68 | 44.6 (+) |
| 2 | 3-F | 15 | 27.3 (+) |
| 3 | 4-F | 15 | 52.8 (+) |
| 4 | 5-F | 46 | 52.8 (+) |
| 5 | 6-F | 73 | 26.3 (+) |
| 6 | 5-Cl | 50 | **55.6** (+) |
| 7 | 4,5-$F_2$ | NR | NA |
| 8 | 5-CN | NR | NA |
| 9 | 4-Ar[a] | 13 | 44.0 (+) |
| 10 | 5-Ar[a] | 14 | 34.0 (+) |

[a] Ar = 4′-$CF_3C_6H_4$. [b] Chiralcel OD 8.7 min (+), 9.8 min (−).

maintaining the standard phenyl substitution at $R_1$, $R_2$, and $R_3$ and holding $R_4$ constant as 2-naphthoyl, our optimum $R_4$ group. We used trifate **1** to screen the $R_5$ substituents, and the results are collected in Table 5.

We chose electron-withdrawing groups for this ligand screen, reasoning that the electronics of the benzo ring would be similar to the other aryl groups on phosphorus, where those types of groups were preferred. The most striking result is the generally reduced yields for these ligands. Entry 3 with the 4-fluoro ligand gave **2** in only 15% isolated yield. It is interesting that *four m*-fluorines are well tolerated in catalysis when they are on the pendant aryl groups on phosphorus, yet *a single m*-fluorine on the benzo ring nearly stops catalysis completely. This same trend was generally observed throughout, and two fluorines or a cyano group do turn off catalysis. The ligand that gives the best yield at 73% (6-fluoro, entry 5) also gives the lowest enantioselectivity at 26%. This ligand showed rotamers in the NMR, and may populate a conformation that is good for turnover and bad for enantioselection. The biphenyl-type ligands (entries 9 and 10) were created to "mimic" a halogen, as strongly electron-deficient aromatic rings are roughly equivalent to a fluoro or chloro substituent directly attached to the ring in terms of $\sigma_p$ Hammett parameters.[13] Their application here was quite disappointing, however, furnishing the product in poor yield and enantioselectivity. The best ligand from this screening set was the 5-chloro derivative, which showed an increase in ee of 11% relative to the unsubstituted system, although the isolated yield was again somewhat diminished. We therefore prepared[5c] ligand **20** possessing four 3,5-difluorophenyl groups (Figure 11), the 5-chloro benzo sub-

(13) (a) Hansch, C.; Leo, A.; Taft, R. W. *Chem. Rev.* **1991**, *91* (2), 165−195. (b) Hansch, C.; Leo, A.; Unger, S. H.; Kim, K. H.; Nikaitani, D.; Lien, E. J. *J. Med. Chem.* **1973**, *16* (11), 1207−1216. (c) Hansch, C.; Leo, A. *Substituent Constants for Correlation Analysis in Chemistry and Biology*; Wiley: New York, 1979.

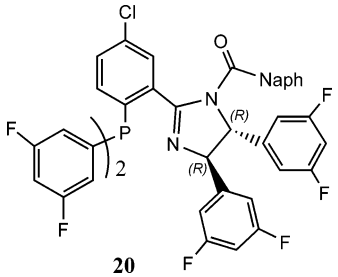


**20**

**FIGURE 11.** Ligand **20**.

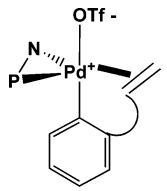


**FIGURE 12.** Tbp geometry.

stituent, and 2-naphthoyl at $R_4$. This ligand was then screened against Heck substrates **1** and **14**. In both cases, no product was formed, even at elevated temperature. It seems likely that this highly electron-deficient ligand has exceeded an electronic limit required for a competent catalyst in the AHR.

**Origin of Enantioselection.** It is not possible to state with certainty why electron-deficient ligands lead to higher enantioselectivity in the AHR, yet the results obtained with the BIPI ligands do allow for speculation on the origin of enantioselection. Overman[14a] has correctly pointed out the possible role of pentacoordinate Pd geometry for this transformation. Numerous pentacoordinate Pd(II) and Pt(II) alkene complexes have been characterized crystallographically.[14b,c] There are two primary forces[14b,d,e] which drive the change from square planar to trigonal bipyramidyl (tbp) geometry in these systems: (1) steric compression in the ligand plane and (2) electron-withdrawing substituents on the metal. This latter effect applies both to the ligand[14b,e] and to the olefin.[14b,d] Current crystallographic data strongly suggest that the geometry shown in the simplified structure of Figure 12 above would be most likely, where the bidentate ligand and the olefin are in the equatorial plane, while the aryl substituent and the triflate occupy the apical positions. It is important to remember that the high asymmetric induction observed with the BIPI ligands occurs only in *nonpolar* solvents, and enantioselection is dramatically eroded in polar media. It is therefore likely that the triflate anion remains closely associated with cationic Pd(II) under these conditions.

A possible explanation for increased enantioselectivity in the AHR with electron-deficient ligands is therefore formation of a pentacoordinate transition state that is inherently more stereoselective than the square planar system. There is evidence[14b,e] that square planar and tbp M(II) complexes are in equilibrium, and this suggests that fluxional behavior might operate in the catalytic cycle. The optimized BIPI ligands, containing electron-deficient P- and N-termini, might simply spend more time in the pentacoordinate geometry prior to olefin insertion than the more electron-rich ligands do.

The relief of steric compression in the ligand plane that can lead to pentacoordinate geometry is considered to be more dominant than electronic effects in this geometric reorganization. It might therefore be asked why sterically encumbered ligands such as those derived from bis-*tert*-butylethylenediamine or camphordiamine in the present work give only modest enantioselectivity in the AHR. The vast majority of the complexes for which tbp geometry has been observed are N,N-ligands forming a *five-membered* chelate, such as 2,9-dimethyl-1,10-phenanthroline, and 2-iminopyridines. The BIPI and PHOX ligands form *six*-membered chelates, while BINAP forms a *seven*-membered chelate. The driving force to reduce the interligand contacts of square planar geometry by geometric change might therefore be attenuated in these larger chelates, leading to default electronic control of geometric reorganization. This model would also explain the superiority of nonpolar solvents, as pentacoordinate geometry would likely be disfavored in ionizing solvents. Overall, this suggests the possibility for superior ligand design in a future system possessing both electron-deficiency and a five-membered or smaller metal chelate.

## Conclusion

We have explored the electronic requirements for enantioselection in the creation of chiral quaternary centers in the intramolecular asymmetric Heck reaction using a new class of electronically tunable ligands. It has been found for the first time that stereoselectivity increases with decreasing phosphine electron density. The electronic dependence of stereoselection on the embedded diamine is more complex, yet is also maximized with decreased diamine electron density. By combining the best phosphorus and nitrogen substitution patterns as relates to enantioselectivity, optimized ligands have been created that give the highest enantioselectivities reported to date for the most challenging types of asymmetric Heck reactions. The BIPI ligands are currently under broad investigation for electronic effects in asymmetric catalysis.

**Supporting Information Available:** Experimental information containing general and specific procedures, characterization of all new compounds, and crystallographic data for complexes **3** and **4**. This material is available free of charge via the Internet at http://pubs.acs.org.

JO049448Z

(14) (a) Ashimori, A.; Bachand, B.; Calter, M. A.; Govek, S. P.; Overman, L. E.; Poon, D. J. *J. Am. Chem. Soc.* **1998**, *120* (26), 6488−6499. (b) Albano, V. G.; Natile, G.; Panunzi, A. *Coord. Chem. Rev.* **1994**, *133*, 67−114. (c) Garrone, R.; Romano, A. M.; Santi, R.; Millini, R. *Organometallics* **1998**, *17* (20), 4519−4522. (d) Fanizzi, F. P.; Maresca, L.; Nayile, G.; Lanfranchi, M.; Tiripicchio, A.; Pacchioni, G. *J. Chem. Soc., Chem. Commun.* **1992**, 333−335. (e) Groen, J. H.; Delis, J. G. P.; van Leeuwen, P. W. N. M.; Vrieze, K. *Organometallics* **1997**, *16*, 6(1), 68−77.